Chinese Journal of
POLYMER SCIENCE

ARTICLE

https://doi.org/10.1007/s10118-021-2607-y
Chinese J. Polym. Sci. **2021**, *39*, 1299–1309

A Robust Self-healing Polyurethane Elastomer Enabled by Tuning the Molecular Mobility and Phase Morphology through Disulfide Bonds

Hai-Tao Wu[a], Bi-Qiang Jin[a], Hao Wang[a], Wen-Qiang Wu[a], Zhen-Xing Cao[a], Zhao-Yang Yuan[a], Yue Huang[a], Wei-Hang Li[a], Guang-Su Huang[a], Lu-Sheng Liao[b*], and Jin-Rong Wu[a*]

[a] *State Key Laboratory of Polymer Materials Engineering, College of Polymer Science and Engineerng, Sichuan University, Chengdu 610065, China*
[b] *Guangdong Provincial Key Laboratory of Natural Rubber Processing, Agricultural Products Processing Research Institute of Chinese Academy of Tropical Agricultural Sciences, Zhanjiang 524001, China*

Electronic Supplementary Information

Abstract Elastomers with outstanding strength, toughness and healing efficiency are highly promising for many emerging fields. However, it is still a challenge to integrate all these beneficial features in one elastomer. Herein, an asymmetric alicyclic structure adjacent to aromatic disulfide was tactfully introduced into the backbone of polyurethane (PU) elastomer. Specifically, such elastomer (PU-HPS) was fabricated by polycondensing polytetramethylene ether glycol (PTMEG), isophorone diisocyanate (IPDI) and *p*-hydroxydiphenyl disulfide (HPS) *via* one-pot method. The molecular mobility and phase morphology of PU-HPS can be tuned by adjusting the HPS content. Consequently, the dynamic exchange of hydrogen and disulfide bonds in the hard segment domains can also be tailored. The optimized sample manifests outstanding tensile strength (46.4 MPa), high toughness (109.1 MJ/m^3), high self-healing efficiency after fracture (90.3%), complete scratch recovery (100%) and good puncture resistance. Therefore, this work provides a facile strategy for developing robust self-healing polymers.

Keywords Self-healing; Polyurethane; Disulfide bonds; Chain mobility; Phase morphology

Citation: Wu, H. T.; Jin, B. Q.; Wang, H.; Wu, W. Q.; Cao, Z. X.; Yuan, Z. Y.; Huang, Y.; Li, W. H.; Huang, G. S.; Liao, L. S.; Wu, J. R. A robust self-healing polyurethane elastomer enabled by tuning the molecular mobility and phase morphology through disulfide bonds. *Chinese J. Polym. Sci.* **2021**, *39*, 1299–1309.

INTRODUCTION

Self-healing polymers are appealing in emerging fields because they are able to repair physical damages and/or functions, which significantly improve the service lifespan and maintain convenience.[1–3] Therefore, self-healing polymers meet the criteria of sustainable development. Although microcapsules or vascular networks have been used to fabricate repairable elastomers, these materials show fatal disadvantages of limited healing cycles, complicated preparation and deteriorated mechanical properties.[4–6] Currently, attentions have been shifted to develop intrinsic pathways through reversible covalent bonds[7–9] or noncovalent interactions due to their excellent reversibility and sensitive responsiveness to environmental stimuli. There are some examples including disulfide bonds,[10–13] boron ester bonds,[14] hydrogen bonds,[15–22] ionic bonds,[23–27] coordination bonds,[28–30] π-π stacking interactions[31] and host-guest interactions.[32] However, simply utilizing these dynamic bonds to achieve high self-healing efficiency without consideration of mechanical properties and repair conditions can hardly produce materials with practical industrial value.

To address this crucial issue, several intelligent tactics have been proposed to prepare robust self-healing elastomers.[9,33–36] Polyurethane (PU) is a particularly attractive elastomer due to its versatile chemistry and easiness of molecular design by selecting and adjusting different soft and hard segments. To improve the mechanical properties of self-healing PU, tactics such as sacrificial networks,[16,37,38] dynamic hard domain[39] and phase locking[40] are developed. For example, Wu *et al.* embeded sacrificial networks into PU. The characteristic sequential breakage of the different sacrificial networks occurs during deformation, leading to simultaneously enhanced tensile strength (6.81 MPa) and toughness (63.7 MJ/m^3). Meanwhile, the existence of sacrificial bonds endows the material with self-healing ability (90%).[37] Wang *et al.* introduced dynamic hard domain into PU. The dynamic hard domain was featured by low binding energy and sequential dissociation with fast rearrangement, resulting in a tensile strength of 5 MPa, toughness of 65.49 MJ/m^3 and good self-repairability.[39] The dynamic hierarchical hard domains designed by Sun *et al.* endows PU with an outstanding strength (52.4 MPa) and a world-record toughness

* Corresponding authors, E-mail: 276491692@qq.com (L.S.L.)
E-mail: wujinrong@scu.edu.cn (J.R.W.)

Special Issue: Self-Healing Polymeric Materials
Received April 3, 2021; Accepted May 15, 2021; Published online July 29, 2021

(363.8 MJ/m^3), whilst without compromising the self-healing efficiency.[36] Lai *et al.* developed a phase locking strategy to introduce dynamic covalent bonds into hard segments, which has a stimulation response temperature (corresponding to the glass transition temperature ($T_{g(H)}$) of hard phase). The dynamic covalent bonds are locked when the temperature is below the $T_{g(H)}$ of hard phase, leading to high mechanical properties; when the temperature exceeds $T_{g(H)}$ of the hard phase, the dynamic covalent bonds are activated and distributed in a specific phase region, resulting in rapid scratch self-repairing.[40] Despite the significant progresses, these PU elastomers usually involve multi-step synthesis and high healing temperature. Therefore, a one-pot method was proposed to facilely synthesize PU elastomer with moderate healing conditions.[41] The one-pot method is the reaction in which the mixture of polydiol and diol reacts with diisocyanate in one step. Since diols are small molecules, their reactivity with diisocyanate is much higher than those of polydiols. As a result, long hard segments are firstly formed in the one-pot samples.[42] Nevertheless, the molar amount of diisocyanate is excessive, and numerous hard segments with isocyanate as the two terminals can directly react with polydiol and formed short hard segments.[41] Such a combination of both long and short segments can realize highly efficient healing and high strength. Therefore, it is valuable to further explore this facile and viable strategy to access high-performance self-healing elastomers.

Herein, by utilizing the one-pot method, we elaborately designed and successfully fabricated a series of self-healing PU elastomers with an asymmetric alicyclic structure adjacent to aromatic disulfide. Specifically, the target elastomer (PU-HPS) was obtained by polycondensation of polytetramethylene ether glycol (PTMEG), isophorone diisocyanate (IPDI) and *p*-hydroxydiphenyl disulfide (HPS) monomers, as shown in Scheme 1. The molecular mobility and phase morphology of PU-HPS can be tuned by adjusting HPS content, resulting in the optimal exchange efficiency for dynamic hydrogen and disulfide bonds. The optimized sample manifests outstanding tensile strength (46.4 MPa), high toughness (109.1 MJ/m^3), high self-healing efficiency of fractured samples (90.3%), complete scratch recovery (100%) and good puncture resistance. Such a combination of comprehensive properties is advantageous for the practical application of self-healing PU.

EXPERIMENTAL

Materials

Poly(tetramethylene ether glycol) (PTMEG, M_n=2000 g/mol)

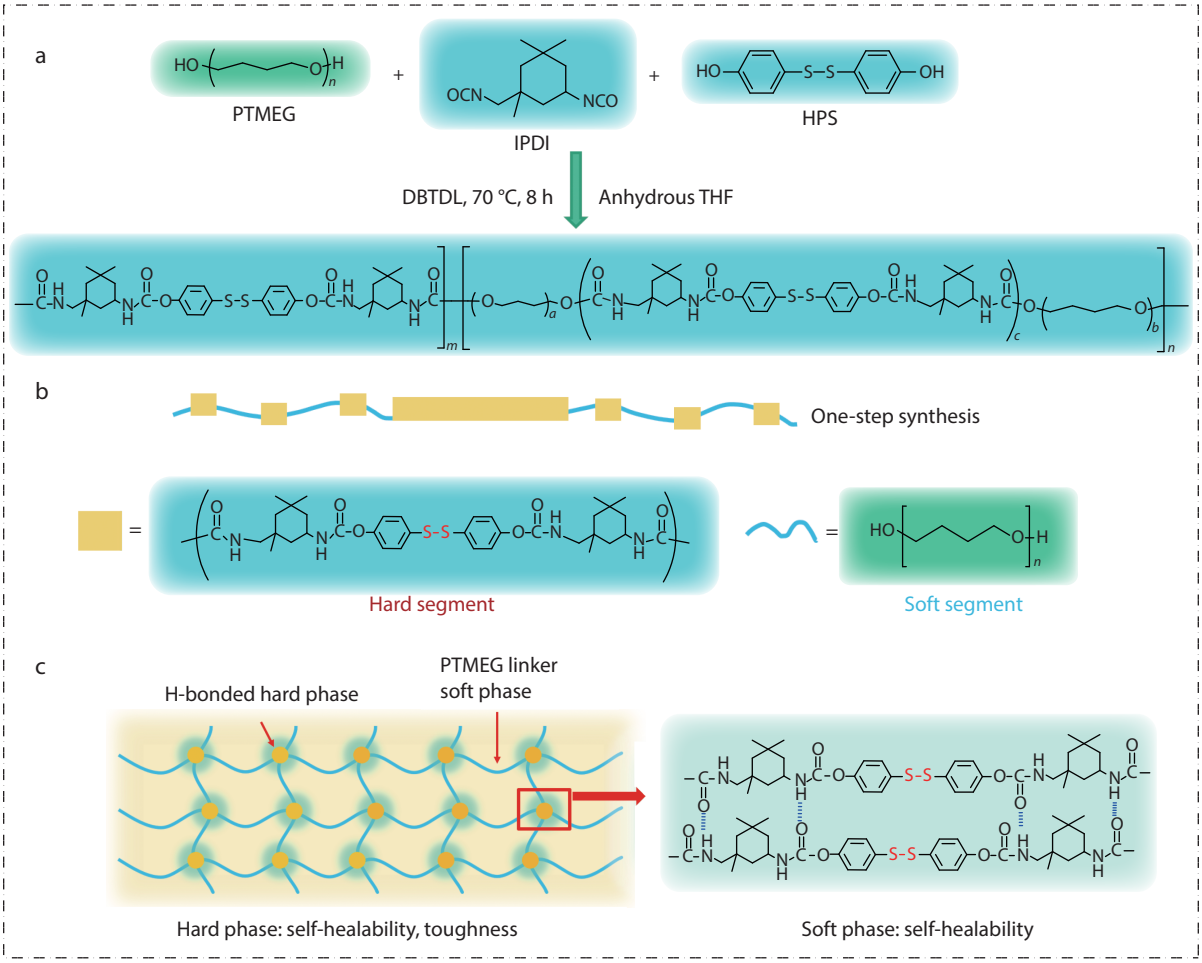

Scheme 1 Molecular design of the target elastomer (PU-HPS). (a) Synthesis route and (b) chemical structure of the PU-HPS; (c) Ideal network structure consisted of soft phase and hard phase.

https://doi.org/10.1007/s10118-021-2607-y

was purchased from Aladdin Chemical Reagent Co., Ltd., and was vacuum drying at 120 °C for 2 h to remove moisture before use. Other reagents were without further purification before use. Isophorone diisocyanate (IPDI, 99%), dibutyltin dilaurate (DBTDL, 95%), anhydrous tetrahydrofuran (THF, 99.5%), and P-hydroxydiphenyl disulfide (HPS, 98%) were purchased from Adamas (China). Dimethyl formamide (DMF, analytical grade) and chloroform ($CHCl_3$, analytical grade) were purchased from Chengdu Lingyun Chemical Reagent Co., Ltd., China.

Synthesis of Resultant PU-HPS

A typical one-pot polymerization procedure for the target PU-HPS is illustrated in Scheme 1(a), and the contents and components information are summarized in Table S1 (in the electronic supplementary information, ESI). Taking PU-HPS-1 as an example, fresh PTMEG (8 g) was poured into a dried three-neck reactor equipped with a magnetic stirrer under N_2 atmosphere, followed by adding IPDI (2.22 g), DBTDL (0.2 mL), HPS (0.076 g) and THF (30 mL). Then, the whole system was heated at 70 °C for 8 h to obtain the complete polymerization. In the end, the product solution was precipitated into excess distilled water and washed for several times, followed by drying in a vacuum at 60 °C for 24 h to constant weight. The wt% ratios of [PTMEG]/[HPS] were varied by 105.3/1 (PU-HPS-1), 32/1 (PU-HPS-2), 21.05/1 (PU-HPS-3), 16/1 (PU-HPS-4) and 10.7/1 (PU-HPS-5) for target elastomers with different disulfide contents.

Preparation of Resultant PU-HPS Film

As-prepared constant weight product (PU-HPS) was dissolved by dioxane in beaker and loaded into a square Teflon mold with the dimensions of 100 mm × 100 mm × 10 mm. The mold was gradually dried under room temperature over 24 h, followed by heating at 60 °C for another 12 h. The residual solvent was removed by vacuum drying at 60 °C for 24 h. A resulting thin film (thickness 0.8 mm) without any bubble could be obtained in this way.

Characterization

FTIR spectra was collected using Thermo Nicolet-is50 FTIR spectrometer fitted with a diamond ATR crystal at room temperature. Temperature-dependent FTIR spectra were recorded in the temperature ranging from 30 °C to 120 °C with a heating rate of 10 °C/min. Raman spectra (DXR, Thermo Fisher Scientific, USA) were performed to confirm characteristic peaks with DXR laser (532 nm). The molecular weight was determined by gel permeation chromatography (GPC), using THF as the eluent. X-ray Diffraction (XRD) analysis was conducted on a PhilipsX'Pert PRO diffractometer (Holland) with Cu Kα radiation (λ=0.154 nm) at room temperature. Atomic force microscopy (AFM) observation was performed on an AIST controller (Association for Iron & Steel Technology Co., Ltd.) in the tapping mode, the test samples were dissolved in THF and dropped on the silicon wafer, and tested directly after solvent volatilization. Dynamic mechanical thermal analysis (DMA, TA Instruments Q800) was performed in tensile mode at a heating and cooling rate of 3 °C/min from −100 °C to 80 °C in a liquid N_2 atmosphere with a frequency of 1 Hz. The stress relaxation mode was performed at different temperatures. Thermogravimetric analysis (TG, 209F1) was performed on a thermo-analyzer instrument from 30 °C to 800 °C under N_2 atmosphere with a heating rate of 10 °C/min. Differential scanning calorimeter (DSC, TA Instruments Q200) test was performed to determine the glass transition temperature (T_g) with a rate of 10 °C/min from −70 °C to 100 °C under N_2 atmosphere. The mechanical properties were measured with a universal testing machine (USA, Instron Instruments, model: 5967), and the tensile speed of 100 mm/min. Each sample was tested for three times. Cyclic tensile test was also performed by conducting successive loaded-unloaded cycles with a maximum strain of 500%. The self-healing test was performed: the dumbbell spline with 0.7 mm thick was cut into two parts by means of fresh blade, immediately spliced together to explore the healing behavior at different time and temperatures. The scratch recovery was observed by an optical microscope (DM4P/Leica, Germany) equipped with a hot stage at different time.

RESULTS AND DISCUSSION

Characterization of Resultant Polymer

The preparation of the target polymer (PU-HPS) containing aromatic disulfide is shown in Scheme 1. The NMR spectra of resultant linear polymers are shown in Fig. S1 (in ESI). ATR-FTIR was employed to record the reaction degree of all synthetic polymers as shown in Fig. 1(a). ATR-FTIR spetra of all of polymers feature negligible bands at 2258 and 3458 cm^{-1}, corresponding to the stretching vibrations of the N=C=O and O−H, respectively.[43] This suggests that the isocyanate and hydroxyl groups are fully converted to urethane bonds. Meanwhile, some new characteristic absorption bands are observed. The bands at 3332 and 1546 cm^{-1} should be attributed to the stretching and bending vibration of N−H, and 1704 cm^{-1} should be ascribed to the C=O stretching vibration.[38] The appearance of these characteristic absorption bands indicates the formation of carbamate groups. Moreover, the strong band at 1102 cm^{-1} is ascribed to the stretching vibration of C−O−C groups in PTMEG chains.[44] S−S and aromatic C−S single bonds show weak signals on the FTIR spectra but can be easily recognized on the Raman spectra. As shown in Fig. 1(b), the absorption bands at 480 and 1100 cm^{-1} are assigned to the stretching vibrations of the S−S and aromatic C−S bonds, respectively.[13,44] Therefore, Raman spectra prove that the disulfide bonds are successfully introduced into the polymers.

To prove the existence of hydrogen bonding interactions, temperature-dependent FTIR measurment was performed. As shown in Fig. 1(c), the bands at 1704 and 1546 cm^{-1} decreasing at elevated temperatures are assigned to the stretching and bending vibration of hydrogen bonded C=O and N−H of urethane groups, respectively. In sharp contrast, the band intensity at 1730 (free C=O groups) and 1525 cm^{-1} (free −NH− groups) increases.[18] Moreover, the intensity at 3332 cm^{-1} (H−bonded N−H) also decreases remarkably, as shown in Fig S2 (in ESI). The results confirm that the hydrogen bonds can dissociate under heating conditions. The presence of hydrogen bonding networks was also demonstrated by conducting solubility experiments. Simply, the PU-HPS-2 films were added into a nonpolar solvent ($CHCl_3$) and a polar solvent (DMF), respectively. The films are fully dissolved in DMF and $CHCl_3$, demonstrating the absence of chemical cross-links and the recyclability by solvent, as shown in Fig. 1(d). It is noteworthy that the DMF solution shows good fluidity, which is caused by the dissociation of hydrogen

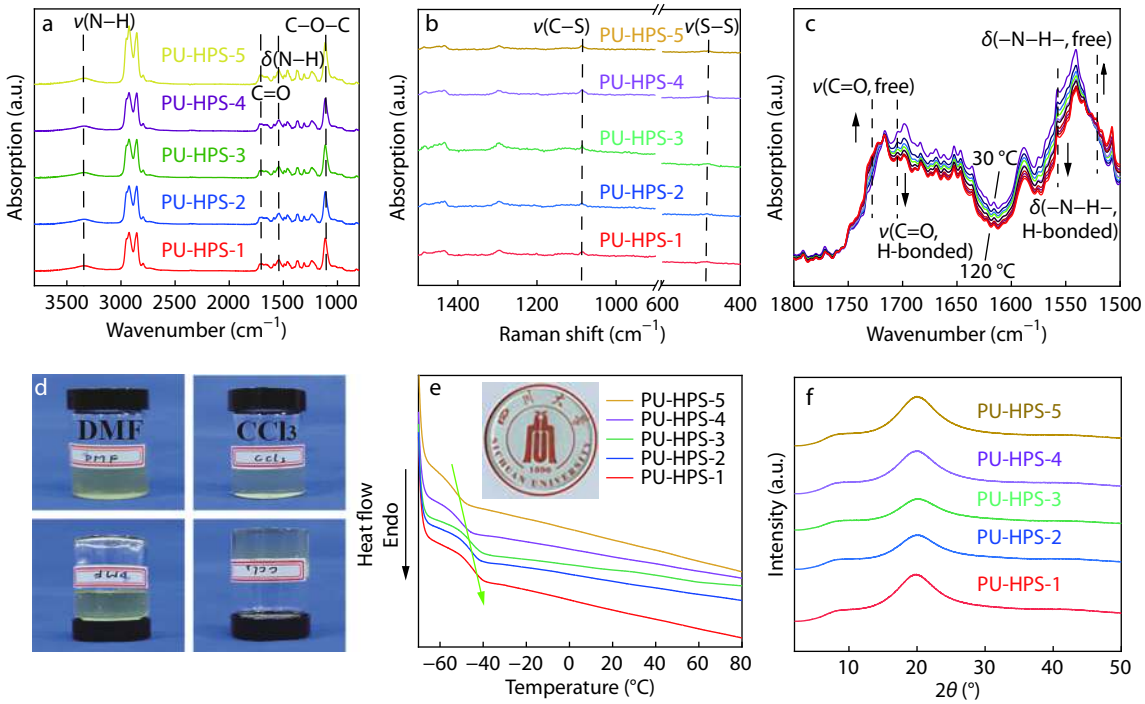

Fig. 1 Structure analysis of the obtained elastomers: (a) ATR-FTIR spectra of PU-HPS; (b) Roman spectra of PU-HPS: the ν(S—S) band around 480 cm^{-1} and the ν(C—S) band at 1100 cm^{-1} are marked; (c) The temperature-dependent FTIR spectra at 1800–1500 cm^{-1} of PU-HPS-2 upon heating from 30 °C to 120 °C; (d) Images of PU-HPS-2 solution in DMF and $CHCl_3$, as well as the corresponding inverted-vial states (concentration is 0.1 g/mL); (e) DSC curves of PU-HPS; (f) XRD patterns of PU-HPS. (The online version is colorful.)

bonds between carbamate groups in the polar solvent. In comparison to the DMF solution, the $CHCl_3$ solution is difficult to flow, suggesting the preservation of hydrogen bonding networks, which is similar to supramolecular gel.[45] Collectively, these results demonstrate the existence of a dynamic but reliable hydrogen bonding network in the as-prepared elastomer.

Thermal Property and Micro-morphology

From the perspective of the molecular design in current system, the thermomechanical behaviors of the resultant PU-HPS play a vital role in determining their mechanical properties. Fig. 1(e) shows the DSC curves of PU-HPS, and the relevant thermal parameters and their corresponding values are summarized in Table S2 (in ESI). It has been reported that aromatic disulfide has a fast exchange rate at room temperature and even at low temperatures.[12,46] Therefore, the T_g value of the soft segments ($T_{g(s)}$) decreases with increasing HPS content. For instance, PU-HPS-5 with [PTMEG]/[HPS]=10.7/1 shows $T_{g(s)}$ of −56.62 °C, which is much lower than −44.42 °C of PU-HPS-1 with [PTMEG]/[HPS]=105.3/1. This phenomenon suggests that the addition of HPS increases the molecular mobility of PU-HPS. Notably, it can be found that all the $T_{g(s)}$ values of the polymers with different HPS compositions are below the room temperature, suggesting that these polymers are classical elastomers rather than plastics at room temperature. It should be noted that neither exothermic nor endothermic peaks are observed on the DSC curves for temperature ranging from −70 °C to 80 °C, indicating noncrystallinity of the elastomers. Meanwhile, the amorphous structure was further verified by X-ray diffraction (XRD) (Fig. 1f). The noncrystalline characteristic is beneficial for achieving high healing efficiency.[47]

It is well-known that because of the thermodynamic incompatibility, the soft and hard segments microphase-separate into soft and hard phases, respectively.[36,38,39] The microphase-separated structure of PU-HPS was observed directly by atomic force microscope (AFM). As shown in Figs. 2(a)–2(e), the AFM images reveal two phases of the soft segments (PTMEG, dark areas) and hard segments (hydrogen bonded aggregates, bright areas). Fig. 2(f) shows a three-dimensional (3D) image of PU-HPS-2. The dark continuous domains in the "trough" represent the PTMEG soft segments, and the lighter dispersed protruding domains with higher surface energy correspond to the hard segments. With the increasing HPS content, the hard domains become sparser and bigger. Specifically, the size of the hard domains increases from 39.5 nm of PU-HPS-1 to 135.2 nm of PU-HPS-5 and the values are summarized in Table S3 (in ESI). Thus, the microphase morphology can be tuned by adjusting the content of HPS, thereby tuning the mechanical and self-healing properties.

Chain Mobility and Dynamic Viscoelastic Properties

To investigate the effect of HPS on the chain mobility of the PU-HPS, the polymers were investigated by DMA in the tensile mode. The storage modulus (E') and loss factor (tanδ) as a function of temperature were plotted in Fig. 3(a). Evidently, the E' and tan δ profiles of the polymers feature two transitions. The transition around −46.57 °C ($T_{g(s)}$) is assigned to the glass transition region of soft segments, while the one around 14.92 °C ($T_{g(H)}$) is the transition of hard segments. The introduction of HPS leads to two evident changes on the

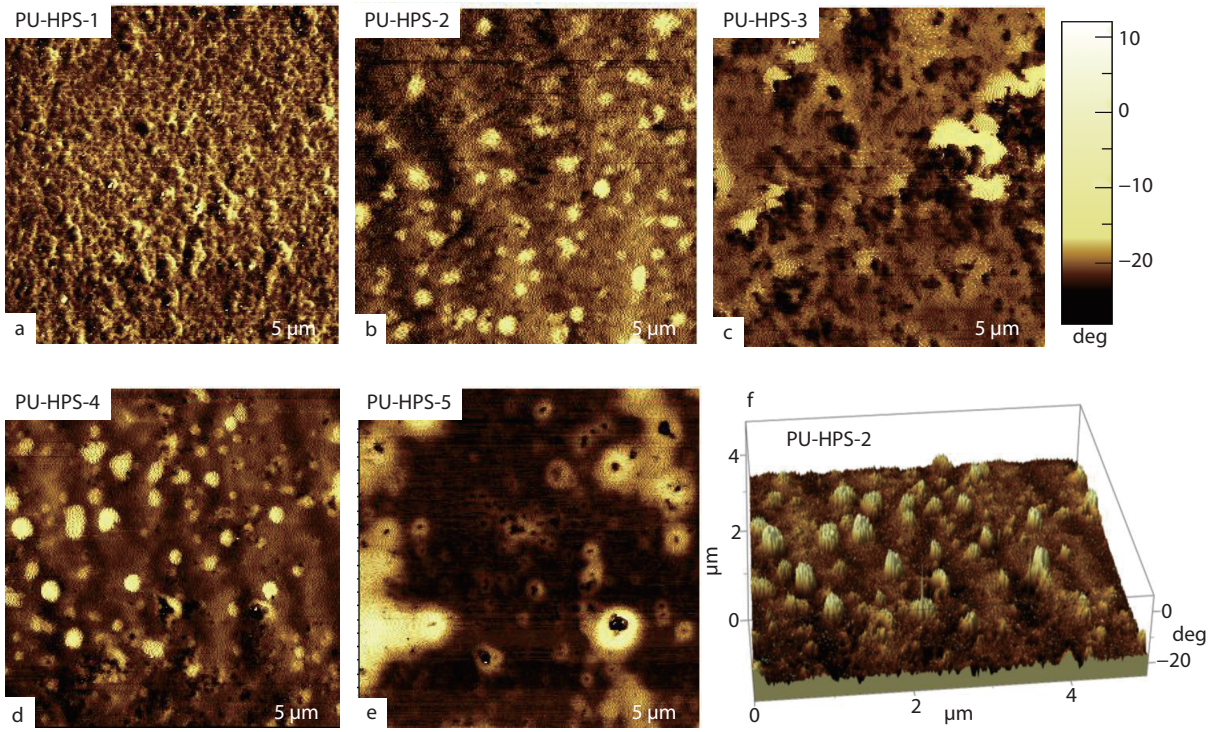

Fig. 2 Atomic force microscopy (AFM) phase images of the resultant PU-HPS: (a) PU-HPS-1, (b) PU-HPS-2, (c) PU-HPS-3, (d) PU-HPS-4 and (e) PU-HPS-5. (f) Three-dimensional (3D) image of PU-HPS-2.

dynamic mechanical spectra. One change is that the E' in the whole tested temperature range decreases with increasing HPS content, the other is that both $T_{g(s)}$ and $T_{g(H)}$ decrease with increasing HPS content. These changes collectively indicate that the introduction of exchangeable disulfide bonds enhances the molecular mobility and deteriorates the stiffness of the PU-HPS, which is conducive to the self-healing performance. Furthermore, for PU-HPS-4 and PU-HPS-5, the absence of a constant plateau of E' above $T_{g(s)}$ indicates that the relaxation of the whole chains takes place due to the exchange of disulfide bonds and the dissociation of hydrogen bonds at elevated temperatures. Such relaxation of the whole chains can also promote the self-healing process.

The time- and temperature-dependent stress relaxation behaviors of PU-HPS were performed to further investigate the chain mobility and dynamic viscoelastic properties. A 10% strain was used, and the relaxation stress was monitored as a function of time at 60 °C. The normalized stress relaxation curves of all of polymers are shown in Fig. 3(b). The gradual decrease of normalized relaxation stress indicate that the PU-HPS can relax stress within an extended time due to the dynamic exchange of hydrogen and disulfide bonds. The relaxation time (τ), which directly reflects the segmental motions and rearrangements of polymers chains, can be considered as the time required for modulus or stress to relax to 36.79% (1/e) of their initial state.[16,37] The τ value decreases with HPS content increasing, indicating that the disulfide bonds can promote exchange rate of hydrogen and disulfide bonds increases. To investigate the effect of temperature on the relaxation dynamics, the normalized stress relaxation curves of all of polymers at different temperatures are presented in Fig. 3(c) and Fig. S3 (in ESI). The stress relaxation becomes faster with increasing temperature. The relaxation time of all polymers is plotted as a function of temperature, as shown in Fig. 3(d). The temperature dependence of the relaxation time can be fitted by the Arrhenius Eq. (1):[16]

$$\ln\tau = \ln\tau_0 + \frac{E_a}{RT} \quad (1)$$

where E_a is activation energy, R and T is gas constant and absolute temperature, respectively. As the disulfide content increases, E_a decreases from 89.2 kJ/mol (PU-HPS-1) to 26.6 kJ/mol (PU-HPS-5). Structurally, the higher the HPS content, the more rapid network rearrangement rate of dynamic networks, which increases the chance of the dynamic bonds to undergo effective collision among the polymer chains, thus achieving lower energy for the exchange reaction. Notably, E_a (81.5 kJ/mol) of the optimized PU-HPS-2 is lower than those of other reported PU systems,[15] indicating that the exchange reactions have lower energy barrier. Such a low energy barrier is beneficial to the recyclability and self-healing of the PU-HPS.

Mechanical Properties

The typical stress-strain curves of PU-HPS are shown in Fig. 4(a), and the corresponding mechanical performances are tabulated in Fig. 4(b) and Table S4 (in ESI). The elastomers exhibit superior mechanical properties after introducing hydrogen and disulfide bonds to form dynamic adaptable networks. For instance, a sample is able to lift two heavy object (1.5 kg) whose weight is more than 15000 times of its own weight (Fig. 4i). We can tune the overall mechanical properties of PU-HPS by adjusting the content of HPS. The tensile strength of the elastomers incre-

https://doi.org/10.1007/s10118-021-2607-y

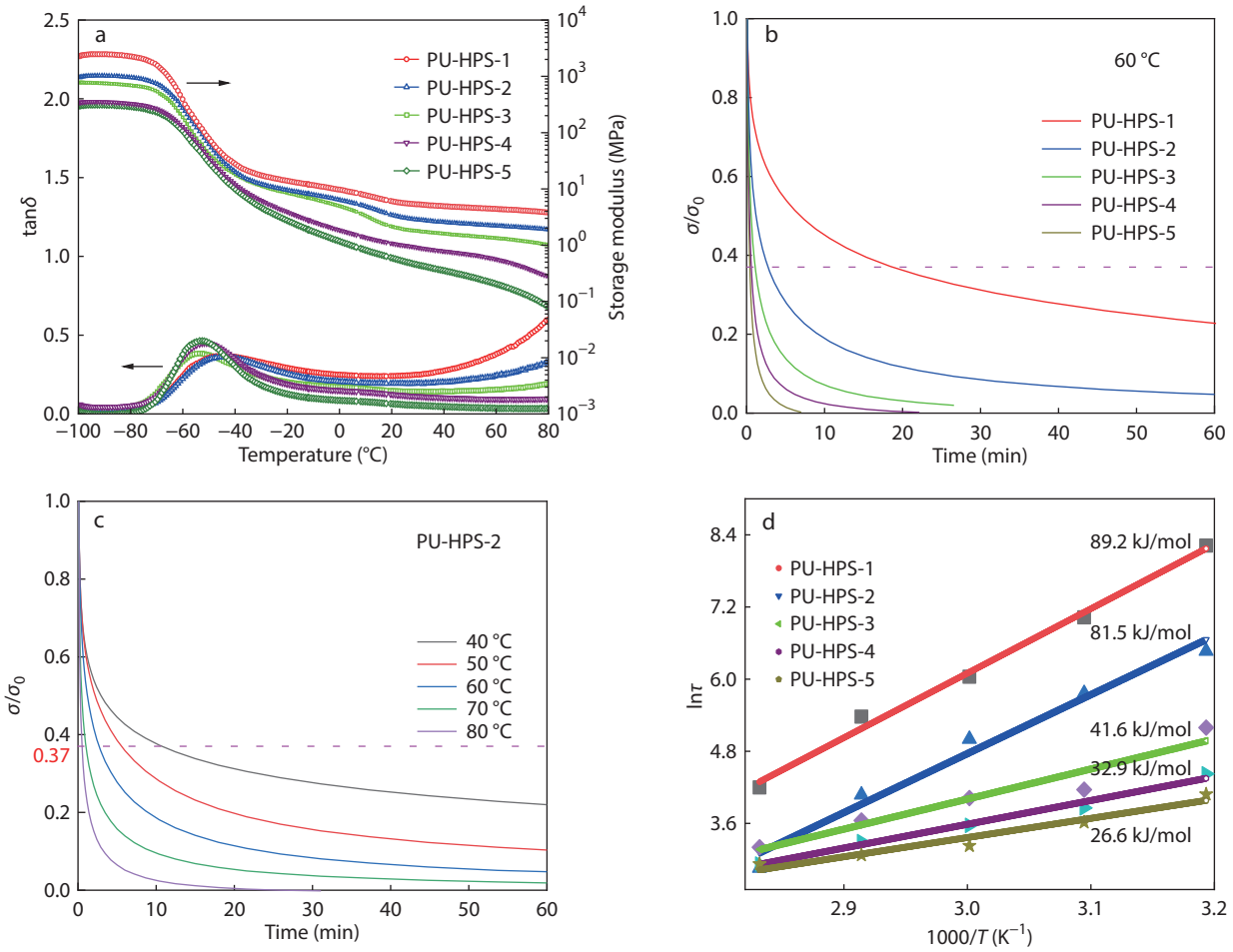

Fig. 3 Dynamic viscoelastic properties. (a) Temperature-dependence of the loss factors and storage modulus of the PU-HPS. (b) Normalized stress-relaxation curves of the PU-HPS at 60 °C. (c) Normalized stress-relaxation curves of the PU-HPS-2 at different temperatures (from 40 °C to 80 °C) for 1 h. (d) Fitting the relaxation time of the PU-HPS according to the Arrhenius's law. (The online version is colorful.)

ases from 6.2 MPa to 46.4 MPa as the HPS content decreases from (0.003 mol, 0.75 g) to (0.0003 mol, 0.08 g). However, the increase of tensile strength is accompanied by a decrease in the strain at break (from 1567% to 655%) and an increase of fracture toughness (from 29.3 MJ/m^3 to 109.1 MJ/m^3). Such a phenomenon is closely related to the chain mobility and phase morphology of PU-HPS. At low HPS contents, the chain mobility is slower, and the hard domains are smaller but denser, which impedes the slippage of the polymer chains and improves the mechanical strength. Therefore, the optimized PU-HPS-2 manifests outstanding tensile strength (46.4 MPa) and toughness (109.1 MJ/m^3). Such mechanical properties are superior to most existing self-healing elastomers and comparable to few strongest self-healing elastomers,[24,35–37,39,41,48–52] as illustrated in Fig. 4(c). To reveal the energy dissipation caused by the dynamic nature of the hydrogen and disulfide bonds, wise-step cyclic tensile tests were performed for the PU-HPS, as shown in Fig. 4(d) and Fig. S4 (in ESI). We calculated the integrated area of the hysteresis loop to quantify the energy dissipation. The hysteresis areas are plotted as a function of the strain in Fig. 4(e). The hysteresis areas are small when the strain is lower than 150%, meaning that the elastomers mainly undergo elastic deformation with the rupture of a small amount of hydrogen and disulfide bonds. The rapid increase of the hysteresis areas with strain indicates that force-induced rupture of hydrogen and disulfide bonds serving as sacrificial bonds contributes to effective energy dissipation.

Generally, the mechanical properties of the elastomer with dynamic bonds are highly dependent on the straining rate. Thus, we performed the tensile tests at various stretching speeds in the range of 10–250 mm/min. Taking PU-HPS-2 as an example, Fig. S5 (in ESI) manifests a unique strain-rate responsive behavior. The tensile strength strikingly increases with increasing strain rate, and meanwhile the Young's modulus obtained from the initial linear region of the stress-strain curves increases from 9.99 MPa to 13.96 MPa. Such a result demonstrates that the PU-HPS possesses a self-stiffening ability with increasing strain rate,[16,53] due to the dynamic characteristic originated from hydrogen and disulfide bonds. Interestingly, the mechanical properties of the PU-HPS are also easily influenced by temperature. Increasing the testing temperature leads to a sharp decrease of tensile strength and an increase of strain at break, as shown in Fig. 4(f). This is because increasing the testing temperature can simultaneously weaken the hydrogen bonding interactions and improve the exchange rate of disulfide bonds, thereby facilitating the unfolding and sliding of the molecular chains. Hence, the

https://doi.org/10.1007/s10118-021-2607-y

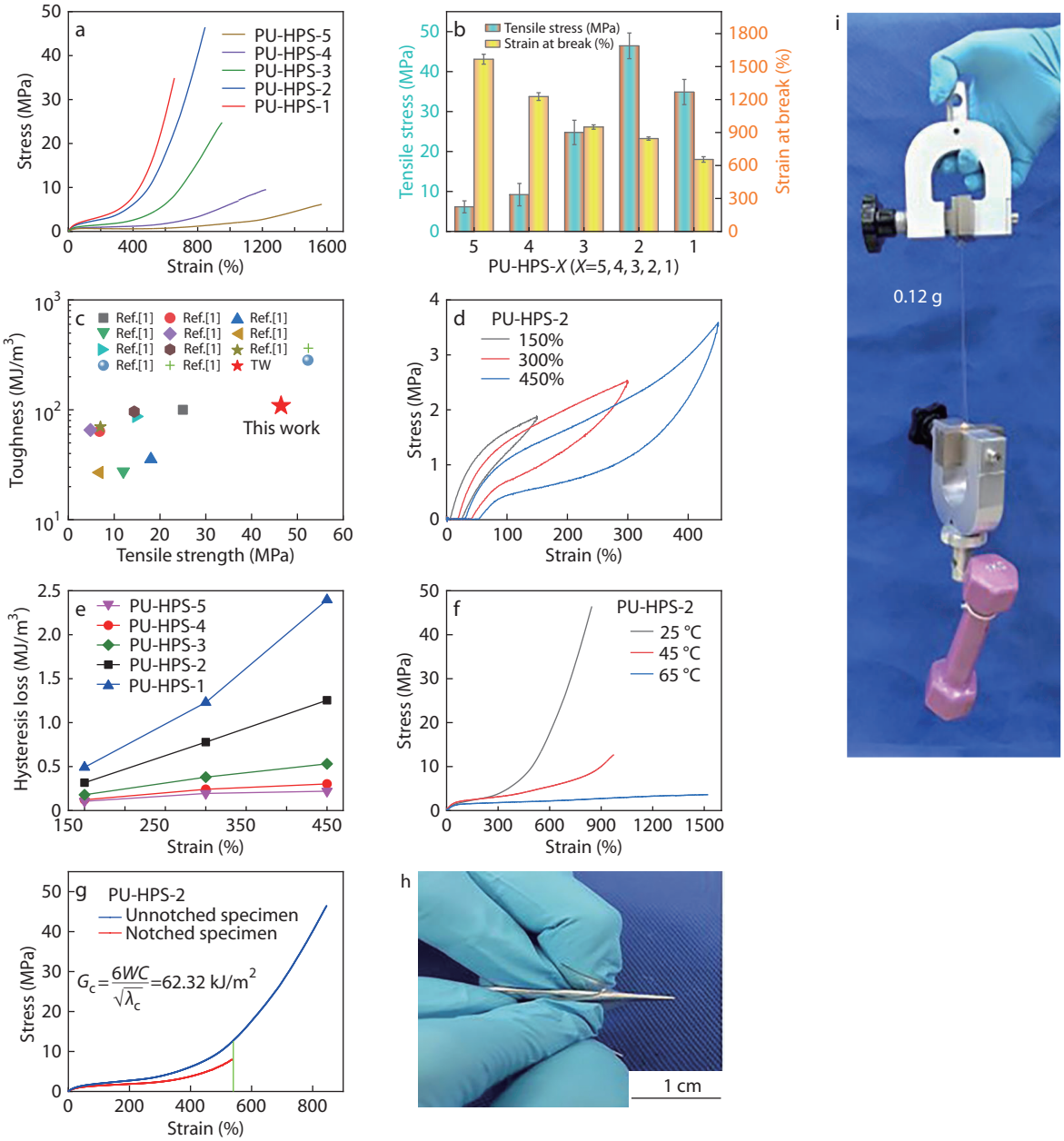

Fig. 4 Mechanical properties of the PU-HPS. (a) Typical stress-strain curves of the resultant elastomers; (b) Summary of resultant elastomers mechanical properties; (c) Comparison of the tensile strength and toughness of PU-HPS-2 with other self-healing elastomers; (d) Cyclic tensile curves of PU-HPS-2 in successive loaded-unloaded cycles with increasing strains but no relaxing time; (e) Corresponding hysteresis area at each loaded–unloaded cycle of PU-HPS; (f) Tensile curves of PU-HPS-2 at different temperatures; (g) Stress-strain curves of notched and non-notched PU-HPS-2 for calculating the fracture energy; (h) Puncture test: the image shows puncture resistance of PU-HPS-2 by pressing the film against the scissors; (i) Two object (1.5 kg) lifted by a film of PU-HPS-2 (0.12 g). (The online version is colorful.)

mechanical properties of the PU-HPS are temperature-dependent, which is similar to those of other reported supramolecular networks.[45]

To test the fracture energy, a notch of 1 mm in length was made in a rectangular PU-HPS-2 sample of about 0.7 mm in thickness and 5 mm in width, the fracture energy was calculated by Greensmith method,[17] and the specific calculation formula was defined as Eq. (2):

$$G_c = \frac{6WC}{\sqrt{\lambda_c}} \quad (2)$$

where C is the notch length; W is the strain energy calculated by integration of the stress-strain curve of an un-notched sample until λ_c; the un-notched sample undergoes a tension process with the same strain rate as the notched sample. As shown in Fig. 4(g) and Fig. S6 (in ESI), the images demonstrate its extraordinary notch-insensitive feature as the notch is not about to propagate even at ~540%, and the fracture energy achieves as high as 62.32 kJ/m^2, which outperforms many reported self-healable materials (Fig. S7 in ESI).[17,40,46,54–56] To prove the ability of PU-HPS to avoid breakage by a sharp object, a puncture test

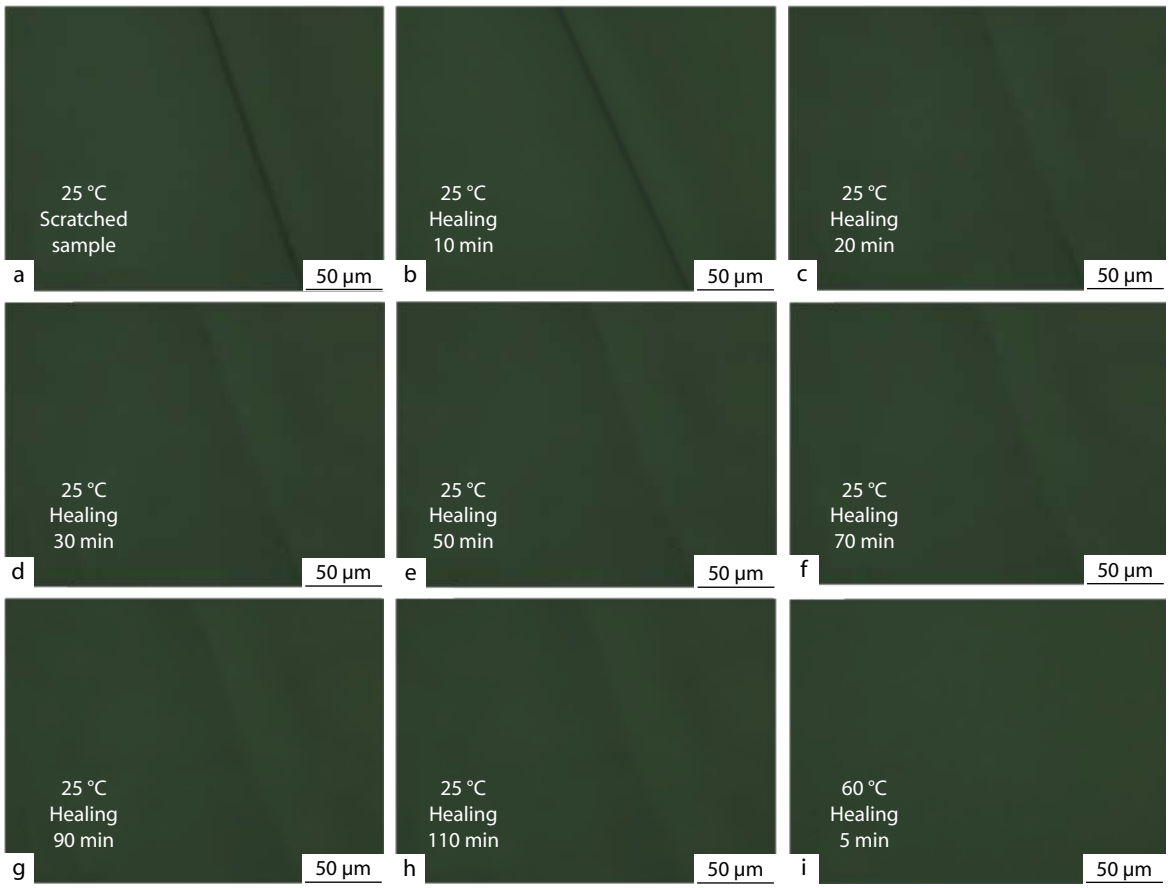

Fig. 5 Optical microscopy images of the scratched PU-HPS-2 film in self-healing process at room temperature: (a) the scratched PU-HPS-2 film Healing 0 min; (b) Healing 10 min; (c) Healing 20 min; (d) Healing 30 min; (e) Healing 50 min; (f) Healing 70 min; (g) Healing 90 min; (h) Healing 110 min; (i) Healing 5 min at 60 °C.

of PU-HPS-2 was performed with scissors to simulate the accidental damage that may occur in daily life. As shown in Fig. 4(h), PU-HPS-2 shows good puncture resistance property.

Self-healing/Recovery Properties

A self-healable ability is key in prolonging the lifetime of materials. In the present work, the dynamic nature of the hydrogen and disulfide bonds, and the good mobility of the soft PTMEG segments can provide PU-HPS with admirable self-healing ability. To reveal this feature, qualitative and quantitative evaluates were performed by optical microscopy and tensile tests, respectively. To qualitatively evaluate the self-healing ability from microscopic scale, we prepared a scratch on a sample film and characterized the evolution of the scratch by means of optical microscope. Fig. 5 depicts the optical microscope images of the scratched PU-HPS-2 film showing a gradual disappearance of the scratch after different healing time at different temperatures. As shown in Figs. 5(a)–5(h), the scratch on the film almost completely disappears after staying at 25 °C for 110 min, indicating an excellent self-healing ability of the PU-HPS. This suggests the hydrogen and disulfide bonds could rapidly exchange between the interfaces at this temperature. When the temperature is further elevated up to 60 °C, the scratch on the film disappears completely within 5 min, indicating the prominent self-healing ability with 100% scratch recovery.

The tensile tests of the PU-HPS before being damaged and after healing were performed to quantitatively evaluate self-healing properties. Typically, the dumbbell-shaped film was cut into two completely separated parts using a fresh razor blade, and then two parts were gently pressed for 30 s and put into an oven at different temperatures for different time. As shown in Fig. 6(a), the reconnected cut dumbbell-shaped sample (0.1 g) can lift a 300 g load after healing 2 h at 60 °C, demonstrating its excellent self-healable behavior. Fig. 6(b) shows the stress-strain curves for the healed PU-HPS-2 after different healing time at different healing temperatures. The self-healing efficiency is quantified by the ratio of the fracture strength of the healed to that of the pristine one. As shown in Fig. 6(b), after being healed at 25 °C for 12 h, the healing efficiency is only 13.3%. In sharp contrast, the healing efficiency further increases to 42.7% and 90.3% after being healed at 60 °C for 12 and 24 h, respectively. Apparently, increasing the healing temperature or proceeding the healing time has positive effects on the promotion of healing efficiency. On one hand, elevated temperature increases the exchange rate of the hydrogen and disulfide bonds and enhances the chain mobility of polymeric chains; on the other hand, prolonging the time allows full chain diffusion across the section interfaces.[16] Both factors can improve the self-healing efficiency to 90.3% after 24 h at 60 °C, which is comparable to those of

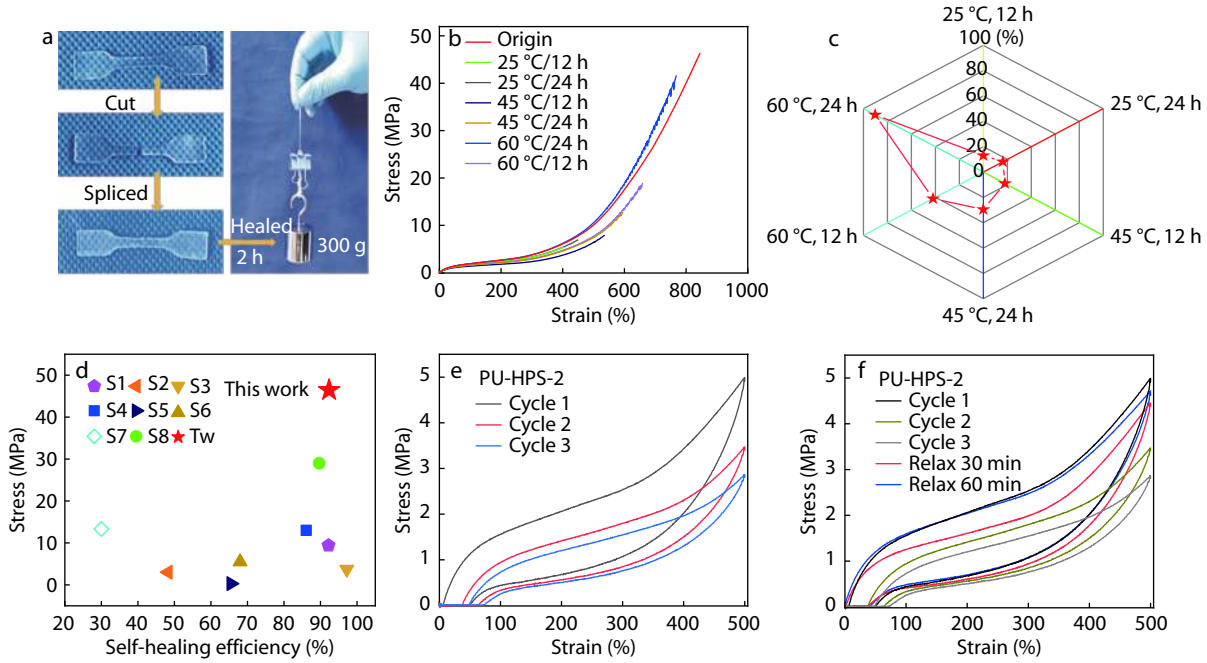

Fig. 6 Self-healing/recovery properties of the PU-HPS. (a) Image shows the healing feature of dumbbell-shaped PU-HPS-2 by cutting into two parts and immediately recombining together for healing 2 h at 60 °C and then lifting a load of 300 g. (b) Stress-strain curves for the healed PU-HPS-2 after different healing time at different temperatures. (c) Summary of self-healing efficiencies of the healed PU-HPS-2. (d) Comparison of self-healing efficiency and mechanical strength among the reported self-healable elastomers at 60 °C. (e) Three successive loaded-unloaded cycles of PU-HPS-2 with a maximum strain of 500%. (f) Cycle tensile curves of PU-HPS-2 with successive three cycles and two additional cycles after relaxing 0.5 h and 1 h, respectively. (The online version is colorful.)

common reported self-healing elastomers,[17,23,57–62] as illustrated in Fig. 6(d).

Furthermore, elastomers in practical use require fast recovery to its mechanical properties after a loading process. Thus, cycle loaded-unloaded test was applied to investigate the self-recovery properties of the PU-HPS. All the polymers were successively loaded-unloaded at a strain of 500% for three continuous cycles (Fig. 6e and Fig. S8 in ESI). After completing the first loaded-unloaded cycle, evident residual strain and large hysteresis are observed in the samples, indicating that the network structure has changed and exhibited a behavior consistent with the typical Mullins effect.[43] In the following two successive cycles, the degree of reduction in tensile strength gradually increases as the cross-linking density decreases derived from the dissociative of hydrogen and disulfide bonds. Further, taking PU-HPS-2 as an example, it was loaded-unloaded to a strain of 500% for three cycles, after which two loaded-unloaded cycles were performed after relaxing for 0.5 and 1 h (Fig. 6f), respectively. Apparently, prolonging the relaxation time leads to the recovery of hydrogen and disulfide bonds, which can be completed after about 1 h. Such a good self-recovery property can be attributed to the re-association of disassociated hydrogen and disulfide bonds during the relaxation process.

CONCLUSIONS

In summary, we designed and successfully fabricated a series of self-healing PU elastomers with an asymmetric alicyclic structure adjacent to aromatic disulfide to tailor the self-healing efficiency and tensile strength. Specifically, such PU elastomer was fabricated by PTMEG, IPDI and HPS *via* one-pot method. The molecular mobility and phase morphology of PU-HPS can be tuned by adjusting the content of HPS. Hard segment domains derived from the asymmetric structure show tunable exchange rate of dynamic hydrogen and disulfide bonds. The optimized sample shows a good balance of mechanical performance (46.4 MPa of tensile strength and 109.1 MJ/m^3 of toughness) and healing efficiency (90.3% in tensile strength), and it also exhibits 100% scratch recovery and good puncture resistance. This advisable strategy illustrates a feasible pathway to combine the robust mechanical performance, great toughness and high healing efficiency in PU elastomer.

Electronic Supplementary Information

Electronic supplementary information (ESI) is available free of charge in the online version of this article at http://doi.org/10.1007/s10118-021-2607-y.

ACKNOWLEDGMENTS

This work was financially supported by the National Natural Science Foundation of China (No. 51873110), the Foundation of Guangdong Provincial Key Laboratory of Natural Rubber Processing and Key Laboratory of Carbon Fiber and Functional Polymers (Beijing University of Chemical Technology), Ministry of Education.

REFERENCES

1 Cordier, P.; Tournilhac, F.; Soulie-Ziakovic, C.; Leibler, L. Self-healing and thermoreversible rubber from supramolecular assembly. *Nature* **2008**, *451*, 977–80.
2 Kang, J.; Tok, J. B. H.; Bao, Z. Self-healing soft electronics. *Nat. Electron.* **2019**, *2*, 144–150.
3 Feng, Z.; Hu, J.; Yu, B.; Tian, H.; Zuo, H.; Ning, N.; Tian, M.; Zhang, L. Environmentally friendly method to prepare thermo-reversible, self-healable biobased elastomers by one-step melt processing. *ACS Appl. Polym. Mater.* **2019**, *1*, 169–177.
4 White, S.R.; Sottos, N. R.; Geubelle, P. H.; Moore, J. S.; Kessler, M. R.; Sriram, S. R.; Brown, E. N.; Viswanathan, S. Autonomic healing of polymer composites. *Nature* **2001**, *409*, 794–797.
5 Hager, M. D.; Greil, P.; Leyens, C.; Van Der Zwaag, S.; Schubert, U. S. Self-healing materials. *Adv. Mater.* **2010**, *22*, 5424–5430.
6 Mookhoek, S. D.; Blaiszik, B. J.; Fischer, H. R.; Sottos, N. R.; White, S. R.; Van der Zwaag, S. Peripherally decorated binary microcapsules containing two liquids. *J. Mater. Chem.* **2008**, *18*, 5390–5394.
7 Chakma, P.; Konkolewicz, D. Dynamic covalent bonds in polymeric materials. *Angew. Chem. Int. Ed.* **2019**, *58*, 9682–9695.
8 Zhang, Z. P.; Rong, M. Z.; Zhang, M. Q. Polymer engineering based on reversible covalent chemistry: a promising innovative pathway towards new materials and new functionalities. *Prog. Polym. Sci.* **2018**, *80*, 39–93.
9 Hu, J.; Mo, R.; Sheng, X.; Zhang, X. A self-healing polyurethane elastomer with excellent mechanical properties based on phase-locked dynamic imine bonds. *Polym. Chem.* **2020**, *11*, 2585–2594.
10 Wang, H.; Liu, H. C.; Zhang, Y.; Xu, H.; Jin, B. Q.; Cao, Z. X.; Wu, H. T.; Huang, G. S.; Wu, J. R. A triple crosslinking design toward epoxy vitrimers and carbon fiber composites of high performance and multi-shape memory. *Chinese J. Polym. Sci.* **2021**, *39*, 736–744.
11 Fortman, D. J.; Snyder, R. L.; Sheppard, D. T.; Dichtel, W. R. Rapidly reprocessable cross-linked polyhydroxyurethanes based on disulfide exchange. *ACS Macro Lett.* **2018**, *7*, 1226–1231.
12 Black, S. P.; Sanders, J. K.; Stefankiewicz, A. R. Disulfide exchange: exposing supramolecular reactivity through dynamic covalent chemistry. *Chem. Soc. Rev.* **2014**, *43*, 1861–1872.
13 Liu, Q.; Liu, Y.; Zheng, H.; Li, C.; Zhang, Y.; Zhang, Q. Design and development of self-repairable and recyclable crosslinked poly(thiourethane-urethane) *via* enhanced aliphatic disulfide chemistry. *J. Polym. Sci.* **2020**, *58*, 1092–1104.
14 Zhang, X.; Wang, S.; Jiang, Z.; Li, Y.; Jing, X. Boronic ester based vitrimers with enhanced stability *via* internal boron-nitrogen coordination. *J. Am. Chem. Soc.* **2020**, *142*, 21852–21860.
15 Xu, J.; Chen, J.; Zhang, Y.; Liu, T.; Fu, J. A fast room-temperature self-healing glassy polyurethane. *Angew. Chem. Int. Ed.* **2021**, *60*, 7947–7955.
16 Wu, H.; Jin, B.; Wang, H.; Wu, W.; Cao, Z.; Wu, J.; Huang, G. A degradable and self-healable vitrimer based on non-isocyanate polyurethane. *Front. Chem.* **2020**, *8*, 585569.
17 Wu, J.; Cai, L. H.; Weitz, D. A. Tough self-healing elastomers by molecular enforced integration of covalent and reversible networks. *Adv. Mater.* **2017**, *29*, 1702616.
18 Wang, H.; Liu, H.; Cao, Z.; Li, W.; Huang, X.; Zhu, Y.; Ling, F.; Xu, H.; Wu, Q.; Peng, Y.; Yang, B.; Zhang, R.; Kessler, O.; Huang, G.; Wu, J. Room-temperature autonomous self-healing glassy polymers with hyperbranched structure. *Proc. Natl. Acad. Sci. U. S. A.* **2020**, *117*, 11299–11305.
19 Song, Y.; Liu, Y.; Qi, T.; Li, G. L. Towards dynamic but supertough healable polymers through biomimetic hierarchical hydrogen-bonding interactions. *Angew. Chem. Int. Ed.* **2018**, *57*, 13838–13842.
20 Liang, Z.; Huang, D.; Zhao, L.; Nie, Y.; Zhou, Z.; Hao, T.; Li, S. Self-healing polyurethane elastomer based on molecular design: combination of reversible hydrogen bonds and high segment mobility. *J. Inorg. Organometal. Polym. Mater.* **2020**, *31*, 683–694.
21 Zuo, H.; Liu, Z.; Zhang, L.; Liu, G.; Ouyang, X.; Guan, Q.; Wu, Q.; You, Z. Self-healing materials enable free-standing seamless large-scale 3D printing. *Sci. China Mater.* **2021**, *64*, 1791–1800.
22 Chen, S.; Bi, X.; Sun, L.; Gao, J.; Huang, P.; Fan, X.; You, Z.; Wang, Y. Poly(sebacoyl diglyceride) cross-linked by dynamic hydrogen bonds: a self-healing and functionalizable thermoplastic bioelastomer. *ACS Appl. Mater. Interfaces* **2016**, *8*, 20591–20599.
23 Peng, Y.; Yang, Y.; Wu, Q.; Wang, S.; Huang, G.; Wu, J. Strong and tough self-healing elastomers enabled by dual reversible networks formed by ionic interactions and dynamic covalent bonds. *Polymer* **2018**, *157*, 172–179.
24 Miwa, Y.; Kurachi, J.; Kohbara, Y.; Kutsumizu, S. Dynamic ionic crosslinks enable high strength and ultrastretchability in a single elastomer. *Commun. Chem.* **2018**, *1*, 5.
25 Zhang, L.; Xiong, H.; Wu, Q.; Peng, Y.; Zhu, Y.; Wang, H.; Yang, Y.; Liu, X.; Huang, G.; Wu, J. Constructing hydrophobic protection for ionic interactions toward water, acid, and base-resistant self-healing elastomers and electronic devices. *Sci. China Mater.* **2021**, *64*, 1780–1790.
26 Xiong, H.; Zhang, L.; Wu, Q.; Zhang, H.; Peng, Y.; Zhao, L.; Huang, G.; Wu, J. A strain-adaptive, self-healing, breathable and perceptive bottle-brush material inspired by skin. *J. Mater. Chem. A* **2020**, *8*, 24645–24654.
27 Zhang, L.; Wang, H.; Zhu, Y.; Xiong, H.; Wu, Q.; Gu, S.; Liu, X.; Huang, G.; Wu, J. Electron-donating effect enabled simultaneous improvement on the mechanical and self-healing properties of bromobutyl rubber ionomers. *ACS Appl. Mater. Interfaces* **2020**, *12*, 53239–53246.
28 Lai, J. C.; Jia, X. Y.; Wang, D. P.; Deng, Y. B.; Zheng, P.; Li, C. H.; Zuo, J. L.; Bao, Z. Thermodynamically stable whilst kinetically labile coordination bonds lead to strong and tough self-healing polymers. *Nat. Commun.* **2019**, *10*, 1164.
29 Li, C. H.; Zuo, J. L. Self-healing polymers based on coordination bonds. *Adv. Mater.* **2020**, *32*, e1903762.
30 Liu, Z.; Zhang, L.; Guan, Q.; Guo, Y.; Lou, J.; Lei, D.; Wang, S.; Chen, S.; Sun, L.; Xuan, H.; Jeffries, E. M.; He, C.; Qing, F. L.; You, Z. Biomimetic materials with multiple protective functionalities. *Adv. Funct. Mater.* **2019**, *29*, 1901058.
31 Burattini, S.; Colquhoun, H. M.; Fox, J. D.; Friedmann, D.; Greenland, B. W.; Harris, P. J.; Hayes, W.; Mackay, M. E.; Rowan, S. J. A self-repairing, supramolecular polymer system: healability as a consequence of donor-acceptor *π*-*π* stacking interactions. *Chem. Commun.* **2009**, 6717–6719.
32 Miyamae, K.; Nakahata, M.; Takashima, Y.; Harada, A. Self-healing, expansion-contraction, and shape-memory properties of a preorganized supramolecular hydrogel through host-guest interactions. *Angew. Chem. Int. Ed.* **2015**, *54*, 8984–8987.
33 Wei, H.; Yang, Y.; Huang, X.; Zhu, Y.; Wang, H.; Huang, G.; Wu, J. Transparent, robust, water-resistant and high-barrier self-healing elastomers reinforced with dynamic supramolecular nanosheets with switchable interfacial connections. *J. Mater. Chem. A* **2020**, *8*, 9013–9020.
34 Yang, S.; Wang, S.; Du, X.; Du, Z.; Cheng, X.; Wang, H. Mechanically robust self-healing and recyclable flame-retarded polyurethane elastomer based on thermoreversible crosslinking network and multiple hydrogen bonds. *Chem. Eng. J.* **2020**, *391*, 123544.
35 Wang, Y.; Huang, X.; Zhang, X. Ultrarobust, tough and highly stretchable self-healing materials based on cartilage-inspired noncovalent assembly nanostructure. *Nat. Commun.* **2021**, *12*, 1291.
36 Wang, X.; Zhan, S.; Lu, Z.; Li, J.; Yang, X.; Qiao, Y.; Men, Y.; Sun, J. Healable, recyclable, and mechanically tough polyurethane

elastomers with exceptional damage tolerance. *Adv. Mater.* **2020**, *32*, e2005759.
37 Wu, B.; Liu, Z.; Lei, Y.; Wang, Y.; Liu, Q.; Yuan, A.; Zhao, Y.; Zhang, X.; Lei, J. Mutually-complementary structure design towards highly stretchable elastomers with robust strength and autonomous self-healing property. *Polymer* **2020**, *186*, 122003.
38 Yao, Y.; Xu, Z.; Liu, B.; Xiao, M.; Yang, J.; Liu, W. Multiple H-bonding chain extender-based ultrastiff thermoplastic polyurethanes with autonomous self-healability, solvent-free adhesiveness, and AIE fluorescence. *Adv. Funct. Mater.* **2020**, *31*, 2006944.
39 Wang, D.; Xu, J.; Chen, J.; Hu, P.; Wang, Y.; Jiang, W.; Fu, J. Transparent, mechanically strong, extremely tough, self-recoverable, healable supramolecular elastomers facilely fabricated *via* dynamic hard domains design for multifunctional applications. *Adv. Funct. Mater.* **2019**, *30*, 1907109.
40 Lai, Y.; Kuang, X.; Zhu, P.; Huang, M.; Dong, X.; Wang, D. Colorless, transparent, robust, and fast scratch-self-healing elastomers *via* a phase-locked dynamic bonds design. *Adv. Mater.* **2018**, *30*, e1802556.
41 Ying, W. B.; Yu, Z.; Kim, D. H.; Lee, K. J.; Hu, H.; Liu, Y.; Kong, Z.; Wang, K.; Shang, J.; Zhang, R.; Zhu, J.; Li, R. W. Waterproof, highly tough, and fast self-healing polyurethane for durable electronic skin. *ACS Appl. Mater. Interfaces* **2020**, *12*, 11072–11083.
42 Krol, P. Synthesis methods, chemical structures and phase structures of linear polyurethanes. Properties and applications of linear polyurethanes in polyurethane elastomers, copolymers and ionomers. *Prog. Mater. Sci.* **2007**, *52*, 915–1015.
43 Luo, M. C.; Zeng, J.; Xie, Z. T.; Wei, L. Y.; Huang, G.; Wu, J. Impact of hydrogen bonds dynamics on mechanical behavior of supramolecular elastomer. *Polymer* **2016**, *105*, 221–226.
44 Liu, M.; Zhong, J.; Li, Z.; Rong, J.; Yang, K.; Zhou, J.; Shen, L.; Gao, F.; Huang, X.; He, H. A high stiffness and self-healable polyurethane based on disulfide bonds and hydrogen bonding. *Eur. Polym. J.* **2020**, *124*, 109475.
45 Shi, S.; Peng, X.; Liu, T.; Chen, Y. N.; He, C.; Wang, H. Facile preparation of hydrogen-bonded supramolecular polyvinyl alcohol-glycerol gels with excellent thermoplasticity and mechanical properties. *Polymer* **2017**, *111*, 168–176.
46 Rekondo, A.; Martin, R.; Ruiz de Luzuriaga, A.; Cabañero, G.; Grande, H. J.; Odriozola, I. Catalyst-free room-temperature self-healing elastomers based on aromatic disulfide metathesis. *Mater. Horiz.* **2014**, *1*, 237–240.
47 Fan, C. J.; Huang, Z. C.; Li, B.; Xiao, W. X.; Zheng, E.; Yang, K. K.; Wang, Y. Z. A robust self-healing polyurethane elastomer: from H-bonds and stacking interactions to well-defined microphase morphology. *Sci. China Mater.* **2019**, *62*, 1188–1198.
48 Hu, J.; Mo, R.; Jiang, X.; Sheng, X.; Zhang, X. Towards mechanical robust yet self-healing polyurethane elastomers *via* combination of dynamic main chain and dangling quadruple hydrogen bonds. *Polymer* **2019**, *183*, 121912.
49 Fan, C. J.; Wen, Z. B.; Xu, Z. Y.; Xiao, Y.; Wu, D.; Yang, K. K.; Wang, Y. Z. Adaptable strategy to fabricate self-healable and reprocessable poly(thiourethane-urethane) elastomers *via* reversible thiol-isocyanate click chemistry. *Macromolecules* **2020**, *53*, 4284–4293.
50 Kim, S. M.; Jeon, H.; Shin, S. H.; Park, S. A.; Jegal, J.; Hwang, S. Y.; Oh, D. X.; Park, J. Superior toughness and fast self-healing at room temperature engineered by transparent elastomers. *Adv. Mater.* **2018**, *30*, 1705145.
51 Zhang, L.; Liu, Z.; Wu, X.; Guan, Q.; Chen, S.; Sun, L.; Guo, Y.; Wang, S.; Song, J.; Jeffries, E. M.; He, C.; Qing, F. L.; Bao, X.; You, Z. A Highly efficient self-healing elastomer with unprecedented mechanical properties. *Adv. Mater.* **2019**, *31*, e1901402.
52 Xu, S.; Sheng, D.; Zhou, Y.; Wu, H.; Xie, H.; Tian, X.; Sun, Y.; Liu, X.; Yang, Y. A dual supramolecular crosslinked polyurethane with superior mechanical properties and autonomous self-healing ability. *New J. Chem.* **2020**, *44*, 7395–7400.
53 Wu, Q.; Xiong, H.; Peng, Y.; Yang, Y.; Kang, J.; Huang, G.; Ren, X.; Wu, J. Highly stretchable and self-healing "solid-liquid" elastomer with strain-rate sensing capability. *ACS Appl. Mater. Interfaces* **2019**, *11*, 19534–19540.
54 Kuhl, N.; Bode, S.; Bose, R. K.; Vitz, J.; Seifert, A.; Hoeppener, S.; Garcia, S. J.; Spange, S.; van der Zwaag, S.; Hager, M. D.; Schubert, U. S. Acylhydrazones as reversible covalent crosslinkers for self-healing polymers. *Adv. Funct. Mater.* **2015**, *25*, 3295–3301.
55 Zhang, Z. P.; Rong, M. Z.; Zhang, M. Q. Mechanically robust, self-healable, and highly stretchable "living" crosslinked polyurethane based on a reversible C-C bond. *Adv. Funct. Mater.* **2018**, *28*, 1706050.
56 Ying, H.; Zhang, Y.; Cheng, J. Dynamic urea bond for the design of reversible and self-healing polymers. *Nat. Commun.* **2014**, *5*, 3218.
57 Yuan, C. e.; Rong, M. Z.; Zhang, M. Q. Self-healing polyurethane elastomer with thermally reversible alkoxyamines as crosslinkages. *Polymer* **2014**, *55*, 1782–1791.
58 Wang, Y.; Guo, Q.; Su, G.; Cao, J.; Liu, J.; Zhang, X. Hierarchically structured self-healing actuators with superfast light- and magnetic-response. *Adv. Funct. Mater.* **2019**, *29*, 1906198.
59 Lee, J.; Tan, M. W. M.; Parida, K.; Thangavel, G.; Park, S. A.; Park, T.; Lee, P. S. Water-processable, stretchable, self-healable, thermally stable, and transparent ionic conductors for actuators and sensors. *Adv. Mater.* **2020**, *32*, e1906679.
60 Jiang, Z.; Tan, M. L.; Taheri, M.; Yan, Q.; Tsuzuki, T.; Gardiner, M. G.; Diggle, B.; Connal, L. A. Strong, self-healable, and recyclable visible-light-responsive hydrogel actuators. *Angew. Chem. Int. Ed.* **2020**, *59*, 7049–7056.
61 Li, Y.; Li, W.; Sun, A.; Jing, M.; Liu, X.; Wei, L.; Wu, K.; Fu, Q. A self-reinforcing and self-healing elastomer with high strength, unprecedented toughness and room-temperature reparability. *Mater. Horiz.* **2021**, *8*, 267–275.
62 Qin, H.; Zhang, T.; Li, N.; Cong, H. P.; Yu, S. H. Anisotropic and self-healing hydrogels with multi-responsive actuating capability. *Nat. Commun.* **2019**, *10*, 2202.

https://doi.org/10.1007/s10118-021-2607-y